



Heavy metals uptake from aqueous solutions and industrial wastewaters by humic acid-immobilized polymer/bentonite composite: Kinetics and equilibrium modeling

T.S. Anirudhan*, P.S. Suchithra

Department of Chemistry, University of Kerala, Kariavattom, Trivandrum 695 581, India

ARTICLE INFO

Article history:

Received 27 January 2009

Received in revised form 3 October 2009

Accepted 6 October 2009

Keywords:

Humic acid

Polymer/clay composite

Heavy metal ion

Adsorption

Wastewater

Regeneration

ABSTRACT

This study explored the feasibility of utilizing a novel adsorbent, humic acid-immobilized-amine-modified polyacrylamide/bentonite composite (HA-Am-PAA-B) for the adsorption of Cu(II), Zn(II) and Co(II) ions from aqueous solutions. The FTIR and XRD analyses were done to characterize the adsorbent material. The effects of pH, contact time, initial adsorbate concentration, ionic strength and adsorbent dose on adsorption of metal ions were investigated using batch adsorption experiments. The optimum pH for Cu(II), Zn(II) and Co(II) adsorption was observed at 5.0, 9.0 and 8.0, respectively. The mechanism for the removal of metal ions by HA-Am-PAA-B was based on ion exchange and complexation reactions. Metal removal by HA-Am-PAA-B followed a pseudo-second-order kinetics and equilibrium was achieved within 120 min. The suitability of Langmuir, Freundlich and Dubinin-Radushkevich adsorption models to the equilibrium data was investigated. The adsorption was well described by the Langmuir isotherm model. The maximum monolayer adsorption capacity was 106.2, 96.1 and 52.9 mg g⁻¹ for Cu(II), Zn(II) and Co(II) ions, respectively, at 30 °C. The efficiency of HA-Am-PAA-B in removing metal ions from different industry wastewaters was tested. Adsorbed metal ions were desorbed effectively (97.7 for Cu(II), 98.5 for Zn(II) and 99.2% for Co(II)) by 0.1 M HCl. The reusability of the HA-Am-PAA-B for several cycles was also demonstrated.

© 2009 Elsevier B.V. All rights reserved.

1. Introduction

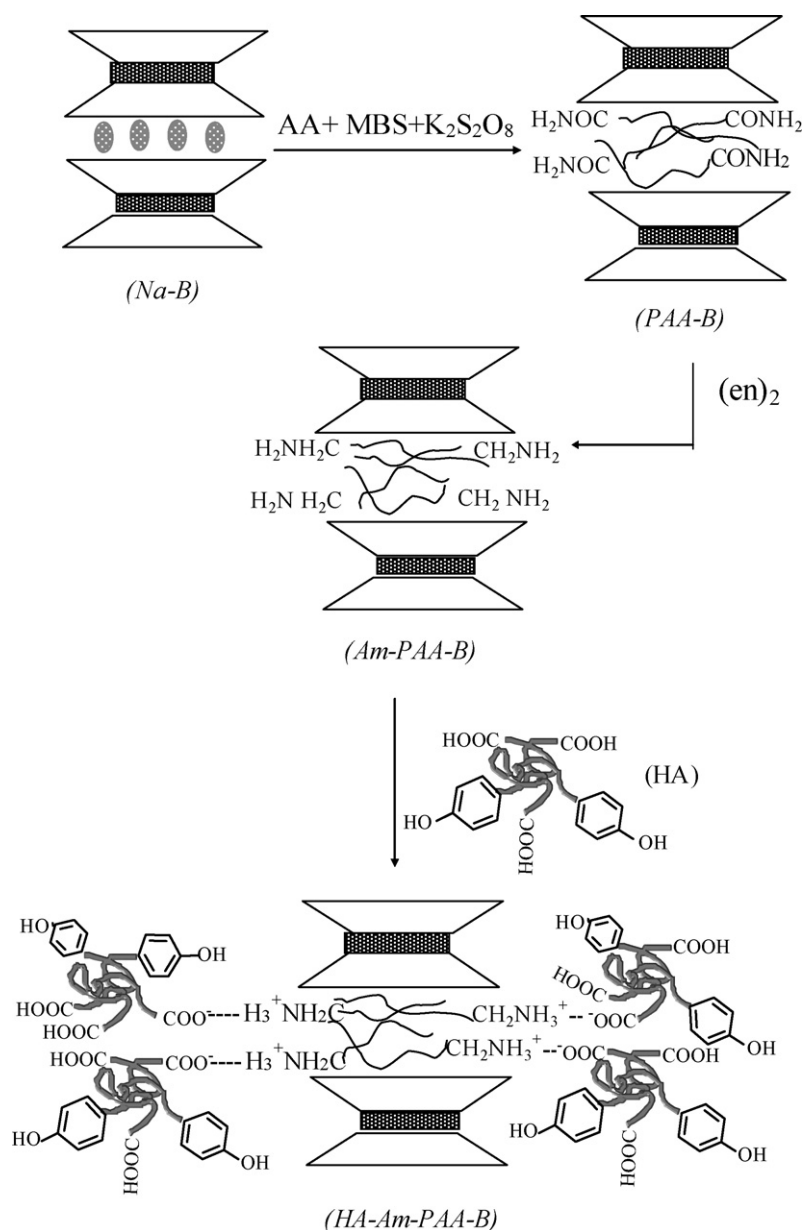
Heavy metals contained in industrial effluents, constitute a major source of metal pollution of the environment, since they are persistent and cannot be degraded or destroyed and can be biomagnified by aquatic organisms. Main industries containing heavy metals in its effluents are mining, metallurgical, nuclear power plants, metal coating, and battery production [1]. Cu(II), Zn(II) and Co(II) ions are among the most common heavy metal ions in industry effluents. The accumulation of these contaminants in human body can cause severe health risk. According to U.S. Environmental Protection Agency (EPA) and WHO, the permissible limit of copper in drinking water is 1.3 and 2.0 mg dm⁻³, respectively [2]. The WHO recommended tolerance limit for Zn(II) is 5.0 mg dm⁻³ [3] while that of Co(II) is limited to 0.05 mg dm⁻³ [4]. Removal of these toxic contaminants is essential for environmental pollution control and many researchers demand a cost effective yet recyclable process such as ion exchange and adsorption for removing heavy metal ions from wastewater. In recent years, solid adsorbents such

as clays, agricultural residues and industrial waste products have been widely used for the removal of heavy metals in low-cost wastewater treatment [5].

Polymer/clay composites have been regarded as promising materials for many applications due to their unique properties, which include high particle dispersion, gas permeability, structural flexibility, fire retardance and thermal and mechanical stability. Although earlier workers [6] have investigated the adsorption performance of polymer/clay composites; a few studies are reported on the recovery of heavy metal ions by using polymer/clay composites. The removal of humic acids (HAs) from water suppliers has demonstrated great attention because (1) they are precursors of potentially calcinogenic chlorinated disinfective by-products in chlorine disinfection process [7] and (2) their high affinity for adsorbing various pollutants including heavy metals and pesticides. Adsorption is an effective and versatile method for the removal of HAs, when combined with an appropriate desorption step solving the problem of sludge disposal. The literature [8] contains several references to the adsorption of HA by various adsorbents which include: activated carbons, zeolites, clay minerals, alumina, resins, chitosan, fly ash, amino polyacrylonitrile fibers and hydrotalcites. In many cases after four or five cycles of repeated use, the adsorbent materials cannot be reused and causes a disposal problem. The

* Corresponding author. Tel.: +91 471 2418782.

E-mail address: tsani@rediffmail.com (T.S. Anirudhan).



Scheme 1. Preparation route of HA-Am-PAA-B.

disposal of the spent adsorbent in an economically sound manner is very important. This study follows from our previous investigation [8], where a polyacrylamide/bentonite composite (PAA-B) with amine functionality (Am-PAA-B) was evaluated as an adsorbent for the removal of HA from aqueous solutions.

HA is one of the major components of humic substances which contain both hydrophilic and hydrophobic molecules as well as many functional groups such as phenolic, carboxylic and hydroxyl groups connected to a skeleton of aliphatic and aromatic units. Because of the deprotonation of carboxylic and phenolic groups in weakly acidic to basic media, HA has negative charge and enhances the adsorption of cations through electrostatic interactions and/or complexation reactions. The acid dissociation constants (pK_a 's) for various carboxylic groups have been reported to be 3.0–5.0. [9]. Lower pH (<3.0) will cause the carboxyl functional groups of HA to be protonated to a higher extent and result in a stronger repulsion for a positively charged cations in the solution. However, at pHs greater than 4.0, the carboxyl groups are deprotonated and favor the adsorption of positively charged cations. Metal ions bind to the

carboxyl groups through ion exchange followed by a complexation reaction. The use of HA-immobilized ion exchange resin for the adsorption of uranium from aqueous solutions was investigated by Ho and Miller [10]. Previously in our groups, we have demonstrated that HA-immobilized bentonite and HA-immobilized zirconium pillared clay can be used as good adsorbents for the removal of some heavy metals and some cationic dyes, respectively, from aqueous solutions [11,12]. The objective of this study is to investigate the efficiency of spent adsorbent, i.e., HA-immobilized Am-PAA-B (HA-Am-PAA-B) for the removal of Cu(II), Zn(II) and Co(II) ions from wastewaters.

2. Experimental

2.1. Materials

The bentonite (B), NNN'N'N''-hexamethylenediamine (HMD) and metal salts ($CuCl_2$, $ZnCl_2$ and $CoCl_2$) were obtained from Fluka, Switzerland. Analytical-grade acrylamide (AA), N,N'-

methylenebisacrylamide (MBA), $K_2S_2O_8$ and ethylenediammine (en) were supplied by E. Merck (India) Ltd. Sodium salt of HA was purchased from Sigma–Aldrich (Germany).

2.2. Preparation of Am-PAA-B

About 10 g of the raw bentonite was stirred for 12 h with 1 L of 1.0 M NaCl solution to replace all exchangeable cations with Na^+ , then centrifuged and washed several times with distilled water until Cl^- was free. The product, Na-saturated bentonite (Na-B) was dried at 105 °C, ground and sieved to obtain –80+230 mesh size particles. To a homogenous suspension of 10 g of Na-B with 250 mL distilled water, 20 g of AA in 50 mL distilled water was added and stirred for 2 h and then 1.6 g MBA and 500 mg $K_2S_2O_8$ followed by 0.5 mL HMD was added to propagate the polymerization and heated in a water bath at 60 °C. The polyacrylamide–bentonite composite obtained was then washed with hot water to eliminate homopolymer. It was dried at 60 °C for 24 h and the product hereafter designated as PAA-B. To introduce the amine functionality in PAA-B, 10 g of PAA-B was heated with 50 mL en at 80 °C and pH 11.0 for 4 h. The product amine-modified PAA-B (Am-PAA-B) was separated from the solution and washed with water until the filtrate was free from en, as indicated by the absence of any blue colour with ninhydrine reagent. The product, Am-PAA-B was dried at 70 °C and sieved to 80–230 mesh size of particles (average diameter of 0.096 mm).

2.3. Preparation of HA-Am-PAA-B

Our earlier work showed that maximum loading of HA onto Am-PAA-B from aqueous solution occurred at an initial pH of 4.0. In order to prepare HA-immobilized Am-PAA-B (HA-Am-PAA-B), 10 g Am-PAA-B was suspended in 100 mL distilled water and 500 mL of 1.25 mmol L^{-1} HA was subsequently added to the suspension. The reaction mixture was then adjusted to pH 4.0 using NaOH and HCl solutions and then stirred continuously for 24 h at room temperature. The product, HA-Am-PAA-B was filtered and washed with water to remove any residual HA and dried at 50 °C and sieved for particle size of 80–230 mesh. Scheme 1 represents the preparatory route of HA-Am-PAA-B.

2.4. Characterization methods of the adsorbent

The X-ray powder diffraction patterns (XRD) of the samples were taken in a Rigaku diffractometer using $Cu K\alpha$ radiation at a scanning speed of 2°min^{-1} . The FTIR spectra were recorded with a Nicolet Protege 460 spectrophotometer between 4000 and 450cm^{-1} using the KBr pellet technique. The cation exchange capacity was determined by ammonium acetate method [13]. The total number of acidic groups and carboxylic groups present in the adsorbent sample was estimated using conductometric titration methods proposed by James et al. [14]. The surface area of the adsorbent was determined using methylene blue adsorption isotherm method. Apparent density of the adsorbent was determined by pycnometric method using nitrobenzene as a displacing liquid using specific gravity bottle. A potentiometric method [15] was used to determine the pH of point of zero charge (pH_{pzc}). The pH of the solution was measured with a Systronic microprocessor pH meter (model μ -362).

2.5. Metal adsorption procedure

A stock solution of 1000mgL^{-1} of Cu(II), Zn(II) and Co(II) ions was prepared in distilled water and corresponding concentration ranges for the experiments were obtained by diluting the stock solution with distilled water. A batch equilibrium technique was

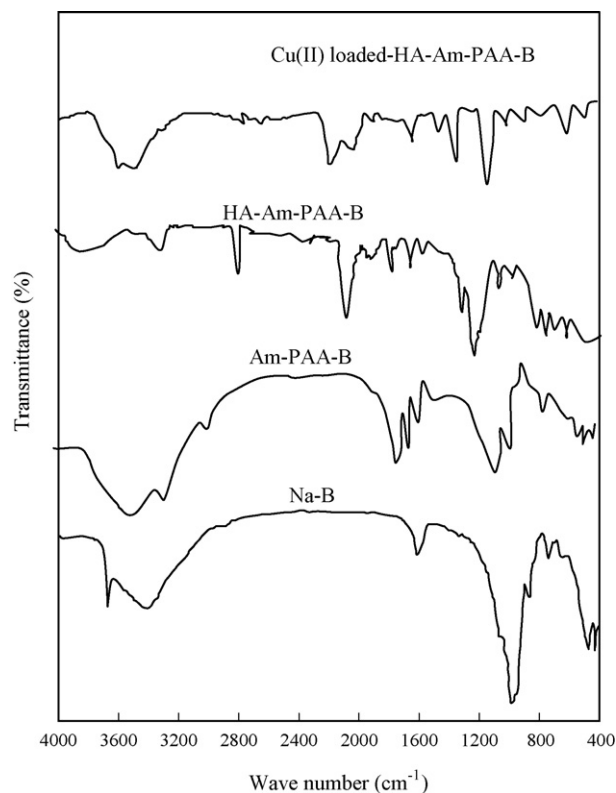


Fig. 1. FTIR spectra of Na-B, Am-PAA-B, HA-Am-PAA-B and Cu(II)-loaded HA-Am-PAA-B.

employed for the investigation of metal uptake by the HA-Am-PAA-B. Fifty milliliter of metal solution containing 0.1 g of the adsorbent in a 100 mL Erlenmeyer flask was agitated at 200 rpm in a temperature controlled water bath shaker (Labline Instruments Pvt. Ltd., Kochi, India) at 30 °C. The initial pH of the solution was adjusted to a definite value using 0.1 M HCl or 0.1 M NaOH solutions. After attaining equilibrium, two phases were separated by centrifugation at 600 rpm for 5 min and an aliquot of the supernatant was analyzed for metal by atomic absorption spectrometry (AAS). A GBC Avanta (A 5450) AAS was used to determine the concentration of Cu(II), Zn(II) and Co(II) ions in aqueous solutions. pH studies were carried out with an initial metal concentration of 25mgL^{-1} in a pH range 2.0–10.0 for Zn(II) and Co(II) and 2.0–6.0 for Cu(II). The effect of ionic strength on metal ion adsorption was studied by conducting batch experiments at different ionic strengths of 0.001, 0.005, 0.01, 0.05 and 0.1 M NaCl and $CaCl_2$. To determine the effect of contact time and adsorbate concentration, 0.1 g adsorbent was added to 50 mL of different metal concentrations ranging from 25 to 100mgL^{-1} and equilibrated for 4 h. Isotherm experiments were performed using different metal concentrations ranged between 10 and 300mgL^{-1} . For desorption studies 0.1 g HA-Am-PAA-B equilibrated with 50 mL of 10mgL^{-1} metal solution and after the adsorption process, the adsorbed metal ions were eluted with different reagents. The eluted adsorbent was then washed thoroughly with distilled water to remove any residual desorbing reagents and placed into metal solution for the subsequent adsorption–desorption cycle.

3. Results and discussion

3.1. Adsorbent characterization

The FTIR spectra of Na-B, Am-PAA-B and HA-Am-PAA-B and Cu(II)-loaded HA-Am-PAA-B are shown in Fig. 1. The spectrum of

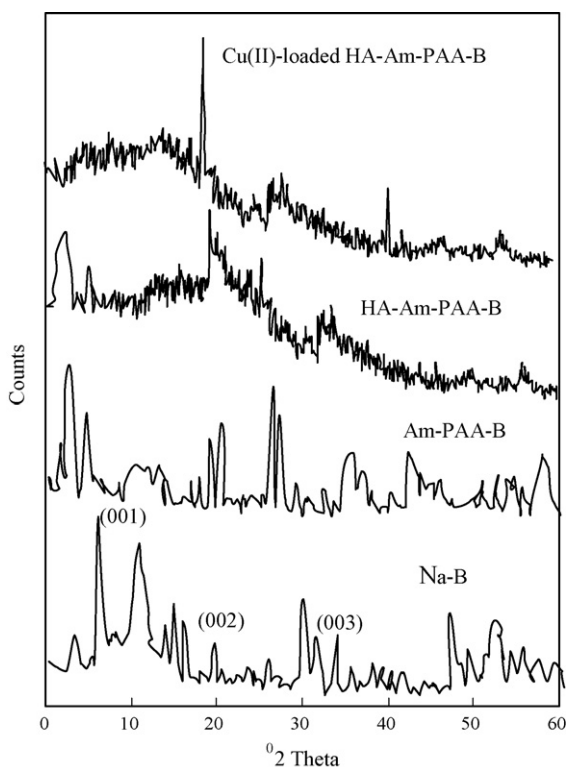


Fig. 2. XRD patterns of Na-B, Am-PAA-B, HA-Am-PAA-B and Cu(II)-loaded HA-Am-PAA-B.

Na-B shows the basic characteristic peaks at 3650 and 3410 cm^{-1} (O–H stretching), 1020 cm^{-1} (Si–O–Si bonds), 760 cm^{-1} (deformation Si–O bond) and 534 and 423 cm^{-1} (bending modes of the Si–O bond). The shifts or change in peaks observed in the spectrum of Am-PAA-B compared to Na-B particularly for asymmetric stretching (from 1024 to 1045 cm^{-1}), deformation (from 760 to 771 cm^{-1}) and bending (from 534 to 543 cm^{-1}) of Si–O–Si bands indicate the interaction of Na-B with PAA. The broader band at 3490 cm^{-1} for the Am-PAA-B spectrum may be due to the N–H stretching vibrations. The presence of two peaks near 1574 and 1030 cm^{-1} was due to N–H bending and C–N stretching provides strong evidence for the presence of amino groups in the Am-PAA-B, while IR spectrum of Na-B did not exhibit these peaks. The formation of a chemical bond between the amino groups on the Am-PAA-B and HA being loaded is indicated by the IR spectrum of HA-Am-PAA-B when N–H bond vibrations (stretching and bending) were formed being shifted to 3976 and 1553 cm^{-1} due to HA immobilization.

In addition, the spectrum of HA-Am-PAA-B shows new bands at 1720 cm^{-1} ($\gamma_{\text{C=O}}$) and 1458 cm^{-1} ($\gamma_{\text{C-O}}$) which are characteristics of the carboxyl (COOH) groups from the immobilized HA from the surface of Am-PAA-B. Moreover, the appearance of four peaks in the region 600 – 900 cm^{-1} , which can be attributed to the polyphenyl groups of HA, is another evidence of the loading of HA onto Am-PAA-B. The characteristic carboxyl bands at 1720 and 1458 cm^{-1} are shifted to 1706 and 1443 cm^{-1} after Cu(II) adsorption. This shifts in peaks observed after metal adsorption, indicate a chemical interaction occurred between Cu(II) ions and carboxylate groups on HA. Moreover the peak at 1368 cm^{-1} is indicative of C–O stretching at the benzene ring when Cu(II) gets coordinated with oxygen. The presence of Cu(II) ions due to adsorption can be confirmed by the band at 517 cm^{-1} of Cu–O stretching vibration in the spectrum of Cu(II)-loaded HA-Am-PAA-B.

The XRD patterns of Na-B, Am-PAA-B, HA-Am-PAA-B and Cu(II)-loaded HA-Am-PAA-B are shown in Fig. 2. The XRD pattern showed that Na-B sample is rich in montmorillonite showing a reflection

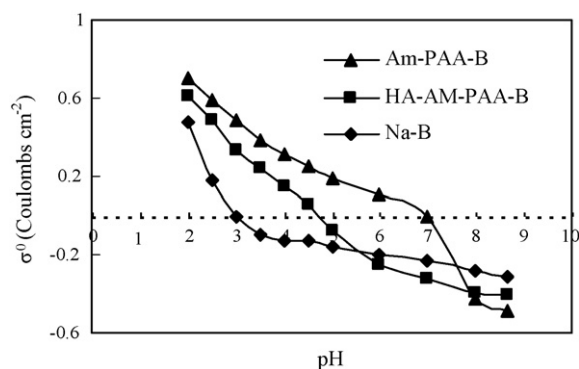


Fig. 3. Surface charge density as a function of pH.

at $2\theta = 5.14^\circ$, which indicates a basal spacing of 1.43 nm . Besides, XRD pattern of Na-B showed the characteristic d values 0.45 , 0.37 , 0.26 and 0.15 nm . The reflection at 0.45 nm further implied 2:1 mineral type. The XRD pattern of Na-B was clearly affected by polymer insertion, as observed by the change of the (001), (002) and (003) reflections. The basal reflection was shifted from 1.53 to 2.49 nm . This increase in basal spacing indicated intercalation of the matrix polymer. The broadening of the (001) reflection indicated that the ordered structure of the layers is disrupted due to the intercalation of the polymer. Loading of HA leads to a considerable decrease in crystallinity in comparison to Am-PAA-B indicated by the decreased number and intensity of reflection. The basal spacing of 3.85 nm in HA-Am-PAA-B suggested the presence of HA. The XRD pattern of Cu(II)-loaded HA-Am-PAA-B shows an increase in 2θ value and a decrease in basal spacing. The diffraction at $2\theta = 5.6^\circ$ with a basal spacing of 2.9 nm in Cu(II)-HA-Am-PAA-B suggested the presence of Cu(II) ions.

Fig. 3 represents the pH dependent surface charge of Na-B, Am-PAA-B and HA-Am-PAA-B. As shown, the Na-B, Am-PAA-B and HA-Am-PAA-B display point of zero charge at pH_{pzc} 3.0 , 7.0 and 4.8 , respectively, suggesting that HA-Am-PAA-B surface is more positive than that of Na-B and more negative than Am-PAA-B surface, since pH above the value of pH_{pzc} the surface charge of the adsorbent has a negative charge, below that pH the clay has a positive charge. The apparent density of Na-B, Am-PAA-B and HA-Am-PAA-B was found to be 1.19 , 1.59 and 1.71 g mL^{-1} , respectively. The total acidity and cation exchange capacity were found to be 0.43 and 0.39 meq g^{-1} for Na-B, and 1.28 and 0.83 meq g^{-1} for HA-Am-PAA-B, respectively. The carboxylate group for HA-Am-PAA-B was found to be 0.66 meq g^{-1} . The surface area of Na-B, Am-PAA-B and HA-Am-PAA-B was found to be 150.3 , 203.5 and $336.3\text{ m}^2\text{ g}^{-1}$, respectively.

3.2. Effect of pH on metal adsorption

Since the surface charge of an adsorbent could be modified by changing pH of the solution, pH is one of the most important parameters affecting the metal adsorption process. The effect of initial pH on the adsorption of Cu(II), Zn(II) and Co(II) ions onto HA-Am-PAA-B is shown in Fig. 4. The results presented show excellent removal capacities for Cu(II), Zn(II) and Co(II) ions by using HA-Am-PAA-B, where a similar profile of removal was observed. For comparison, metal hydroxide precipitation by NaOH is also given in Fig. 4. It can be seen that at any pH, metal removal by adsorption on HA-Am-PAA-B is very much greater than the removal by hydroxide precipitation observed in the absence of adsorbent. With an increase of pH of the solution from 2.0 to 6.0 , Cu(II) removal capacity increased from 30.0 to 99.0% at an initial concentration of 25 mg L^{-1} . Similarly, when the initial pH of suspension increased from 2.0 to

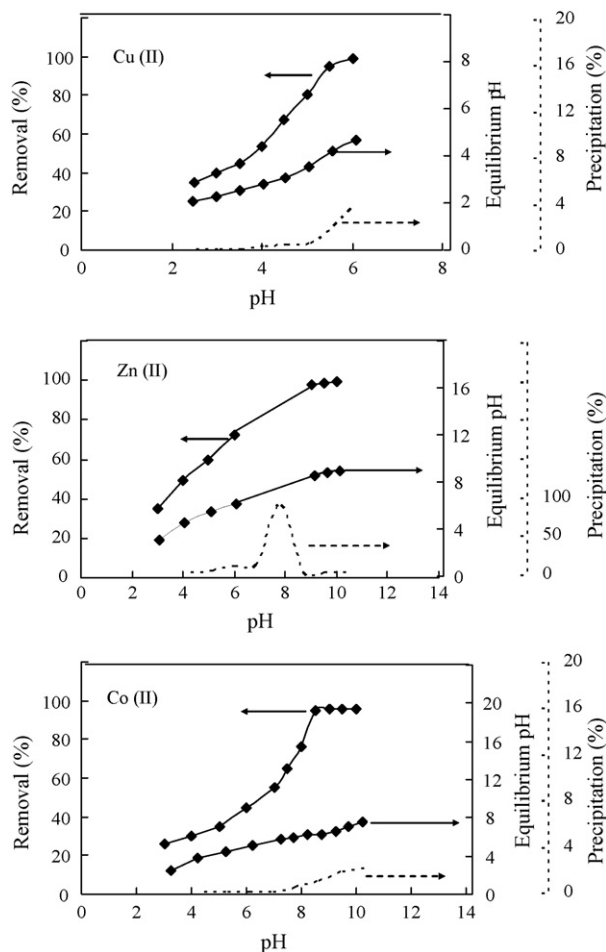


Fig. 4. Effect of pH on the removal of Cu(II), Zn(II) and Co(II) ions onto HA-Am-PAA-B.

10.0, the removal capacity increased from 27.1 to 99.0% for Zn(II) and 22.7 to 95.4% for Co(II) at an initial concentration of 25.0 mg L^{-1} . It has been shown that the final pH is always less than the initial pH (Fig. 4). In the case of Cu(II), when the initial pH of the reaction mixture varied between 3.0 and 6.0, the final pH of the reaction mixture remained between 2.7 and 4.7 for an initial concentration of 25 mg L^{-1} . The possible sites on HA-Am-PAA-B for specific adsorption in acidic pH include H^+ ions in $-\text{COOH}$ functional groups. Divalent Cu(II) ions displaced two protons from $-\text{COOH}$ groups for each metal cations adsorbed while one proton is exchanged for each of the monovalent $(\text{Cu}(\text{OH})^+)$ species adsorbed. At higher pH values (>5.5), the solubility product of $\text{Cu}(\text{OH})_2$ is exceeded, therefore, Cu(II) is removed from the solution by adsorption as well as by precipitation. Thus to correlate Cu(II) removal with adsorption (ion exchange), an optimum initial pH of 5.0 was chosen for performing all subsequent adsorption experiments. For Zn(II) and Co(II), pH 9.0 and 8.0, respectively, was selected to be the optimum initial pH for further studies.

The decreased metal adsorption at low pH can be explained as follows: (i) in acidic region both the adsorbent (since pH_{pzc} of the adsorbent is 4.8, below which the adsorbent surface is positive) and adsorbate are positively charged and the net interaction is that of electrostatic repulsion and (ii) the positively charged metal ions faces a good competition with the higher concentration of H^+ ions present in the reaction mixture and (iii) generally, the carboxyl groups presented a pK_a value between 3.0 and 5.0 [16]. At pH lower than pK_a , carboxylate groups carried positive charge, restricting access sites to metal ions as a result of repulsive forces and resulting in a low uptake. At $\text{pH} < 5.0$, the linked H^+ is released from the

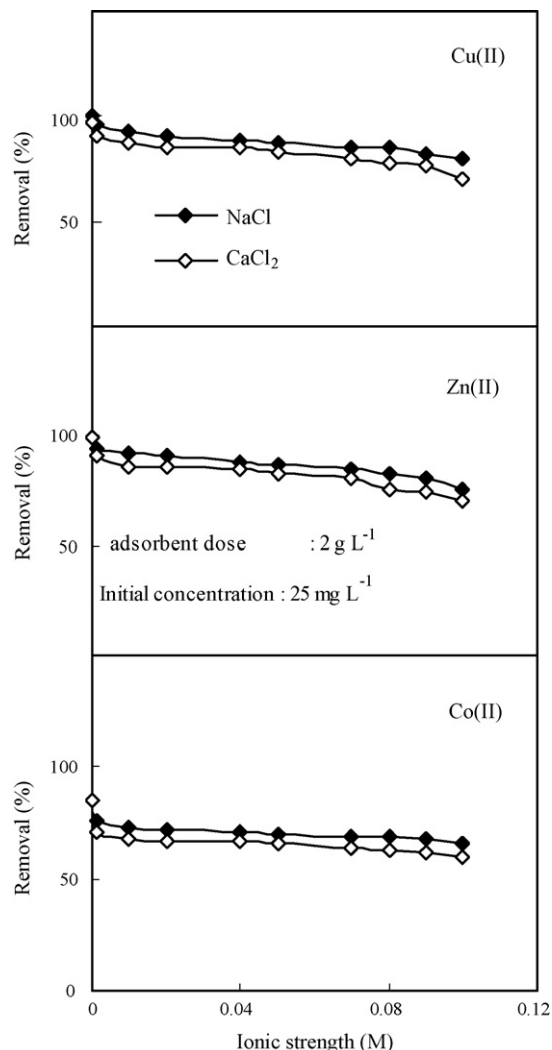


Fig. 5. Effect of ionic strength on the removal of Cu(II), Zn(II) and Co(II) ions onto HA-Am-PAA-B.

active sites and adsorbed amount of metal ions is increased. In this pH range, it is believed that the ion exchange and complex formation process are the major mechanism for removal of metal ions from solution. The amount of metal ions adsorbed by HA-Am-PAA-B increased in the order of $\text{Cu}(\text{II}) > \text{Zn}(\text{II}) > \text{Co}(\text{II})$.

3.3. Effect of ionic strength

Fig. 5 shows the effect of ionic strength on the adsorption behavior of HA-Am-PAA-B towards heavy metal ions. As shown, in the presence of Na- and Ca-electrolyte there was a decrease in adsorption capacity of HA-Am-PAA-B towards metal ions. When ionic strength of both electrolyte increased from 0.001 to 0.1 M, the total decrease in percentage removal of 25 mg L^{-1} Cu(II), Zn(II) and Co(II) was 20.7, 24.5 and 26.3, respectively, for Ca-electrolyte and 16.4, 18.2 and 19.8, respectively, for Na-electrolyte. This suggests that with increase in the concentration of chloride anions in metal ion solution, there is a possibility for the formation of uncharged species (CuCl_2 , ZnCl_2 and CoCl_2) and negatively charged chloride complexes (CuCl_3^- , CuCl_4^{2-} , ZnCl_3^- , ZnCl_4^{2-} , CoCl_3^- and CoCl_4^{2-}) that will invariably reduce the adsorption capacity of the adsorbent [17] for positively charged cations. The adverse effect of ionic strength on metal uptake suggests the possibility of ion exchange mechanism being in operation in the adsorption process. Ca^{2+} and

Na⁺ ions can compete with metal ions for the same binding sites on the HA-Am-PAA-B surface and thus negatively affect the removal efficiency.

3.4. Adsorption kinetics

Kinetic behavior of the adsorbent, towards Cu(II), Zn(II) and Co(II) ions, was examined by monitoring the extent of adsorption with respect to contact time and the time profiles are given in Fig. 6. The adsorption was rapid for all the three metal ions; an interaction period 30 min supplied about 73% adsorption where as the equilibrium was reached in approximately 120 min. After this period, the amount of adsorbed metal ions did not change significantly with time. The rapid uptake of metal ions onto HA-Am-PAA-B may indicate that most of reaction sites of the adsorbent are exposed for interaction with metal ions. The equilibrium time is independent of initial concentrations. The time profile of metal uptake is a single, smooth and continuous curve leading to saturation, suggesting the possible monolayer coverage of metal ions on the surface of the adsorbent. Due to the presence of MBA crosslink units in polymer/clay composite, the adsorbent possesses a high swelling capacity in water [18] and, consequently its network is sufficiently expanded to allow a fast diffusion process for the metal ions. This expanded network of the adsorbent favors the interaction between the cations and the most favorable adsorption sites (carboxylic groups) on the adsorbent surface. Furthermore, this may indicate that there is an ion exchange/complexation reaction between HA from adsorbent surface and metal ions because these ion exchange/complexation reactions are usually very fast as indicated by complexation studies of HA with metal ions [19]. With increase in metal concentration from 25 to 100 mg L⁻¹, the amount of metal adsorbed increased from 11.47 to 47.31 mg g⁻¹ for Cu(II), 11.15 to 44.71 mg g⁻¹ for Zn(II) and 10.98 to 34.37 mg g⁻¹ for Co(II) indicating that the Cu(II) removal by adsorption on HA-Am-PAA-B is concentration dependent. Also, the amount of metal ions adsorbed by the adsorbent is of the following order: Cu(II) > Zn(II) > Co(II) for the concentrations studied.

Two generally applied simplified kinetic models, i.e., pseudo-first-order and pseudo-second-order equations are analyzed to model the adsorption kinetic data [20,21]. The pseudo-first-order model is given by:

$$q_t = q_e(1 - e^{-k_1 t}) \quad (1)$$

where k_1 is the pseudo-first-order rate constants (min⁻¹) and q_e (mg g⁻¹) is the pseudo-equilibrium adsorption corresponding to the initial metal ion concentration C_0 and q_t (mg g⁻¹) is the amount of metal adsorbed at any time t . On the other hand pseudo-second-

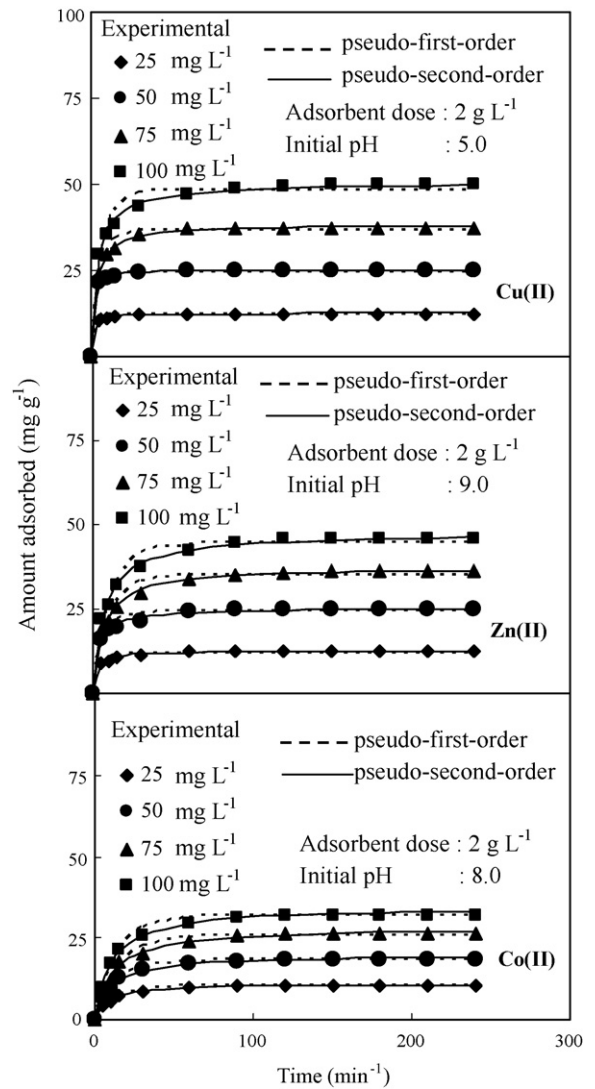


Fig. 6. Adsorption kinetics of Cu(II), Zn(II) and Co(II) ions uptake onto HA-Am-PAA-B.

order model is expressed as

$$q_t = \frac{k_2 q_e^2 t}{1 + k_2 q_e t} \quad (2)$$

where k_2 (g mg⁻¹ min⁻¹) is the pseudo-second-order rate constant. The values of q_e , k_1 and k_2 for different concentrations and

Table 1
Kinetic parameters for the adsorption of Cu(II), Zn(II) and Co(II) ions onto HA-Am-PAA-B.

Metal ion	C_0 (mg L ⁻¹)	q_e (exp)	Pseudo-second-order				Pseudo-first-order			
			k_2 (g mg ⁻¹ min ⁻¹)	q_e (cal)	χ^2	R^2	k_1 (min ⁻¹)	q_e (cal)	χ^2	R^2
Cu(II)	25	11.47	6.83×10^{-2}	11.58	0.06	0.999	0.415	10.79	0.56	0.994
	50	22.52	4.02×10^{-2}	22.43	0.04	0.999	0.316	20.96	0.87	0.987
	75	36.98	0.71×10^{-2}	37.01	0.07	0.999	0.164	34.74	1.67	0.983
	100	47.31	0.39×10^{-2}	47.77	0.94	0.995	0.117	45.67	1.54	0.967
Zn(II)	25	11.15	2.56×10^{-2}	11.38	0.02	0.999	0.159	10.13	0.81	0.982
	50	21.23	1.06×10^{-2}	22.11	0.42	0.995	0.112	20.56	2.57	0.959
	75	35.58	0.32×10^{-2}	36.55	0.89	0.997	0.073	31.23	5.76	0.969
	100	44.71	0.28×10^{-2}	45.18	1.66	0.993	0.057	41.34	4.47	0.968
Co(II)	25	10.98	1.06×10^{-2}	11.07	0.07	0.999	0.075	10.02	0.43	0.961
	50	17.88	0.43×10^{-2}	18.13	0.59	0.997	0.064	16.76	0.72	0.944
	75	25.37	0.28×10^{-2}	25.78	0.15	0.999	0.034	24.47	1.91	0.984
	100	34.37	0.21×10^{-2}	35.17	0.76	0.997	0.046	33.38	1.80	0.931

temperatures were calculated using non-linear regression analysis and the results are shown in Table 1. As shown, on comparison with pseudo-first-order, pseudo-second-order kinetic expression yielded the best results for experimental kinetic data with higher values of R^2 and lower χ^2 values. As shown in Table 1, the value of rate constant k_2 decreases with increasing initial concentration and surface loading. Higher surface loadings would result in less diffusion efficiency and a high competition of metal ions for a fixed reaction sites, consequently a lower k_2 values were observed. Moreover, Fig. 6 also represents the best agreement of the experimental kinetic data with the pseudo-second-order kinetic model.

3.5. Adsorption isotherm

The relation of metal ion concentration in the bulk and the adsorbed amount at the interface is a measure of the position of equilibrium in the adsorption process and can generally be expressed by one or more of a series of isotherm models. The interpretation of adsorption data through theoretical or empirical equations is essential for the quantitative estimation of the adsorption capacity or amount of the adsorbent required to remove the unit mass of pollutant from wastewater. Fig. 7 shows adsorption isotherms of Cu(II), Zn(II) and Co(II) ions at 30 °C. All the three metals' adsorption onto HA-Am-PAA-B was found to be concentration dependent. As calculated from adsorption data, the amount of Cu(II), Zn(II) and Co(II) increased from 4.37 to 107.85, 4.25 to 96.75 and 4.13 to 52.15 mg g⁻¹, respectively, when the initial concentration increased for all the three from 10 to 300 mg L⁻¹. In this study the experimental data were correlated by the non-linear forms of Langmuir, Freundlich and Dubinin-Radushkevich adsorption isotherm equations:

$$\text{Langmuir: } q_e = \frac{Q^0 b C_e}{1 + b C_e} \quad (3)$$

$$\text{Freundlich: } q_e = K_F C_e^{1/n} \quad (4)$$

$$\text{Dubinin-Radushkevich: } q_e = q_m (\varepsilon^2)^{-\beta} \quad (5)$$

where q_e is the quantity of metal adsorbed at equilibrium over the mass of adsorbent material (mg g⁻¹) and C_e is equilibrium concentration (mg L⁻¹) of the adsorbate species in solution. Q^0 and b are Langmuir constants related to the monolayer adsorption capacity (mg g⁻¹) and energy or intensity of adsorption (L mg⁻¹). The Freundlich constants K_F and $1/n$ are related to the adsorption capacity and heterogeneity factors related to binding strength, respectively. q_m is D-R constant related to theoretical saturation capacity and ε is the Polanyi potential, equal to $RT \ln(1 + 1/C_e)$, where R is the gas constant (kJ mol⁻¹ K⁻¹) and T is the temperature (K).

A detailed analysis of the correlation coefficients obtained for these isotherms by using non-linear optimization method for Cu(II), Zn(II) and Co(II) adsorption, showed that all the three isotherm equations adequately describe the adsorption data, but are better fitted to Langmuir, from which we can assume that adsorption of Cu(II), Zn(II) and Co(II) onto HA-Am-PAA-B would not take place beyond a monolayer coverage and all adsorption sites are equivalent with uniform energies of adsorption with out any interaction between the adsorbed molecules. Fig. 7 also shows a comparison between the theoretical Langmuir, Freundlich and D-R isotherms and the experimental data. The resulting parameters for all the three isotherms are tabulated in Table 2. As shown, Q^0 which is indicative of adsorption capacity changed in the order of Cu(II) > Zn(II) > Co(II). Similar results are also reported by earlier workers [22]. The Freundlich exponent $1/n$ gives an indication of the favorability of adsorption. Values of $1/n < 1.0$ represent favorable adsorption condition. The values of $1/n$ obtained in the present study for all the three metal ions are less than unity, indicate the

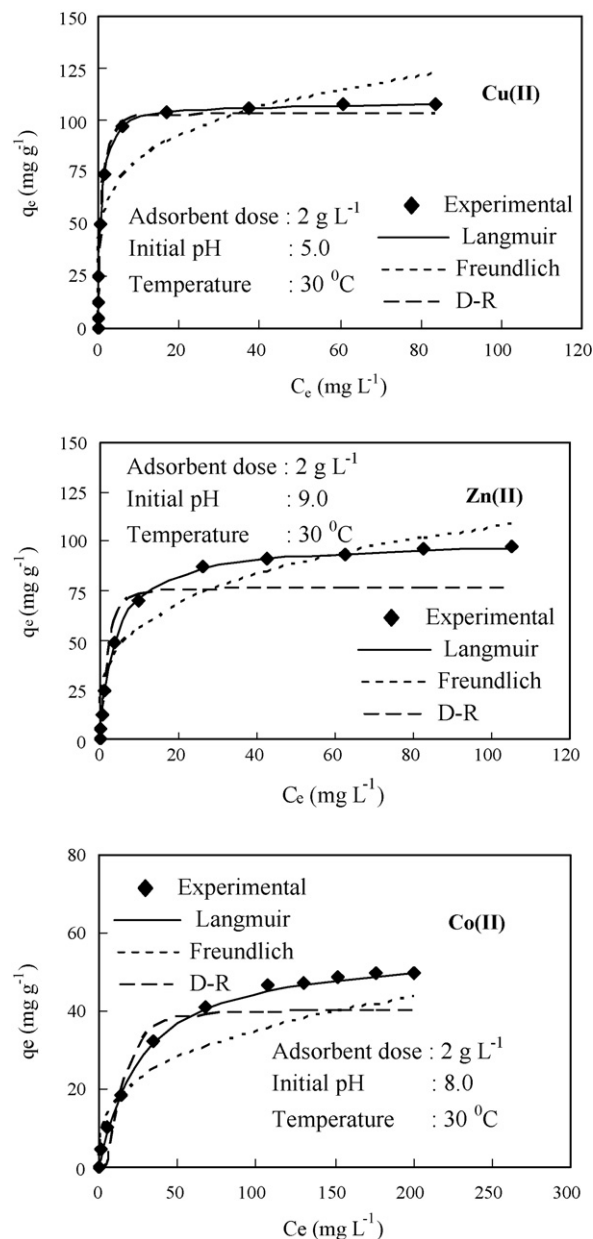


Fig. 7. Comparison of the experimental and model fits of the Langmuir, Freundlich and D-R isotherms for the adsorption of Cu(II), Zn(II) and Co(II) ions onto HA-Am-PAA-B.

favorable adsorption of Cu(II), Zn(II) and Co(II) ions onto HA-Am-PAA-B. The value of D-R constant β is related to the adsorption free energy E (kJ mol⁻¹), which is defined as the free energy change required to transfer 1 mol of ions from solution to the solid surface. From the β values the values of E can be calculated as $E = (2\beta)^{-1/2}$. The magnitude of E is useful to determine the type of adsorption reaction. Physisorption processes have adsorption energy in the range 1–8 kJ mol⁻¹, while chemisorption processes have adsorption energy in the range 20–40 kJ mol⁻¹. On the other hand, adsorption can be explained by ion exchange if E values lie between 8.0 and 16.0 kJ mol⁻¹ [23]. The calculated E values (Table 3) for Cu(II), Zn(II) and Co(II) adsorption onto HA-Am-PAA-B are ranged between 7.87 and 8.46 kJ mol⁻¹ indicating an ion exchange reaction, which support the idea, that the adsorption of metal ions onto HA-Am-PAA-B mainly proceeds by binding surface functional groups, as stated earlier.

Table 2
Isotherm parameters for the adsorption of Cu(II), Zn(II) and Co(II) ions onto HA-Am-PAA-B.

Isotherm parameters	Metalion		
	Co(II)	Cu(II)	Zn(II)
Langmuir			
Q^0 (mg g ⁻¹)	106.21	96.15	52.93
b (L mg ⁻¹)	1.32	0.21	0.03
R^2	0.999	0.999	0.998
χ^2	0.11	0.13	1.46
Freundlich			
K_F	50.43	27.13	7.13
$1/n$	0.191	0.214	0.254
R^2	0.943	0.967	0.978
χ^2	14.75	12.63	11.67
D-R			
q_m	99.45	99.13	38.64
β	0.0067	0.0069	0.0079
R^2	0.933	0.954	0.976
χ^2	6.64	7.56	5.49
E_a (kJ mol ⁻¹)	8.64	8.51	7.96

The Langmuir parameters Q^0 and b are further used to predict the affinity between the metal ions and HA-Am-PAA-B using the dimensionless separation factor $R_L = 1/(1/bC_e)$. The values of R_L indicate the shape of the isotherms to be either unfavorable ($R_L > 1$), linear ($R_L = 1$), favorable ($0 < R_L < 1$) or irreversible ($R_L = 0$) [24]. The values of R_L for Cu(II), Zn(II) and Co(II) adsorption were determined over a wide concentration range at 30 °C and the results confirmed the favorable uptake of Cu(II), Zn(II) and Co(II) onto HA-Am-PAA-B. Also, higher R_L values at lower metal concentrations showed that adsorption was more favorable at lower concentrations.

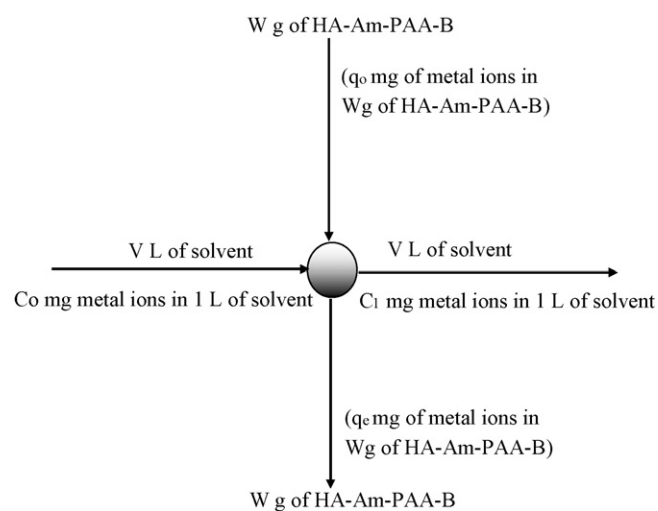
3.6. Design of single stage batch reactor

A single stage batch adsorption system is designed from the adsorption isotherm data, the schematic diagram of which is shown in Scheme 2. The metal solution to be treated contains V (L) of water and an initial metal ion concentration of C_0 (mg L⁻¹), which is to be reduced to C_t (mg L⁻¹) in the end of the adsorption process. During the process when W (g) of HA-Am-PAA-B is added, the metal ion concentration on it is changed from initial q_0 to final q_t . The mass balance equation of metal ion removal from the liquid to that loaded on the adsorbent is:

$$(C_0 - C_t)V = (q_t - q_0)W \quad (6)$$

Table 3
Chemical composition of wastewaters.

Electroplating wastewater for Cu(II)		Industrial estate wastewater for Zn(II)		Nuclear power plant coolant water for Co(II)	
Parameter	Value (mg L ⁻¹)	Parameter	Value (mg L ⁻¹)	Parameter	Value (mg L ⁻¹)
Cu ²⁺	43.30	Zn ²⁺	20.01	Sb(V)	5.01
Ni ²⁺	11.70	Cu ²⁺	20.03	Co(II)	10.03
Na ⁺	314.70	Glucose	1437.51	Fe(III)	30.04
K ⁺	28.80	Urea	107.30	Ni(II)	15.05
Mg	611.41	FeSO ₄ ·7H ₂ O	24.81	Ag(I)	5.00
Ca	43.30	KH ₂ PO ₄	43.85	B(III)	20.07
Cl ⁻	319.90	pH	6.50	Cr(III)	4.00
SO ₄ ²⁻	29.30			Li(I)	0.50
CO ₃ ²⁻	89.90			Cs(I)	0.50
<i>Hardnesses</i>					
CaCO ₃	714.41				
COD	413.31				
pH	5.15				

**Scheme 2.** Design of single stage batch reactor.

When fresh adsorbent is used, $q_0 = 0$ and if the system is allowed to reach equilibrium, then Eq. (6) can be expressed as:

$$\frac{W}{V} = \frac{C_0 - C_e}{q_e} \quad (7)$$

Substituting for q_e from Eq. (3) and rearranging gives

$$\frac{W}{V} = \frac{(C_0 - C_e)(1 + bC_e)}{Q^0 b C_e} \quad (8)$$

Inserting, the Langmuir constants Q^0 and b (Table 2) in Eq. (8):

$$\frac{W}{V} = \frac{(C_0 - C_e)(1 + 1.5C_e)}{165.5C_e} \quad (9)$$

This equation can be used to calculate the mass of HA-Am-PAA-B required to achieve certain percentage removal by treating a definite volume of metal ion containing effluent having an initial concentration C_0 . Fig. 8 represents the experimental and theoretical masses of HA-Am-PAA-B against different volumes for different percentages of removal of Cu(II) ions and mass of HA-Am-PAA-B against different concentrations and different volumes for the removal of Cu(II) ions (>99.0%) from aqueous solutions. The amounts of adsorbent calculated using the model Eq. (9) match those observed experimentally for different volumes of effluent and concentrations.

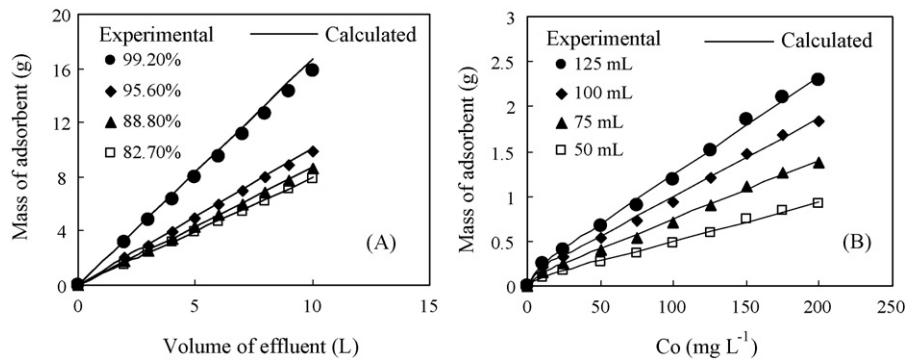


Fig. 8. (A) Mass of HA-Am-PAA-B against different volumes for different percentage of removal of Cu(II) ions and (B) mass of HA-Am-PAA-B against different concentrations and different volumes for removal (>99.0%) of Cu(II) ions from aqueous solutions.

3.7. Test with industrial wastewaters

The utility of the HA-Am-PAA-B as an adsorbent for Cu(II), Zn(II) and Co(II) in presence of other ions was assessed by its application in industrial wastewater treatment. Simulated electroplating industrial wastewater, industrial estate wastewater [25] and nuclear power plant coolant water [26] were used for Cu(II), Zn(II) and Co(II) ions, respectively. The compositions are given in Table 3 and Fig. 9 shows that the amount of adsorbed metal increases with increasing the HA-Am-PAA-B dose. It is because the number of available adsorption sites increases by increasing the adsorbent dose. The results also reveal that the treatment of metal ions in wastewater samples is not significantly different from the results predicted based on single solute batch experiments. Almost complete removal of metals was achieved from 50 mL of each sample of Cu(II), Zn(II) and Co(II) ions with 0.3, 0.4 and 0.5 g of adsorbent, respectively. Thus, the present study demonstrates that HA-Am-PAA-B can be successfully used for the removal of Cu(II), Zn(II) and Co(II) ions from industrial wastewaters.

3.8. Comparison with other adsorbents

The adsorption capacity of HA-Am-PAA-B for Cu(II), Zn(II) and Co(II) ions were compared with those of other adsorbents reported in the literature. Theoretical background makes the monolayer adsorption capacity (Q^0) quite useful and convincing for comparison in liquid phase adsorption. It is found that the adsorption capacity of HA-Am-PAA-B towards Cu(II), Zn(II) and Co(II) (106.21, 96.15 and 52.93 mg g⁻¹ for Cu(II), Zn(II) and Co(II),

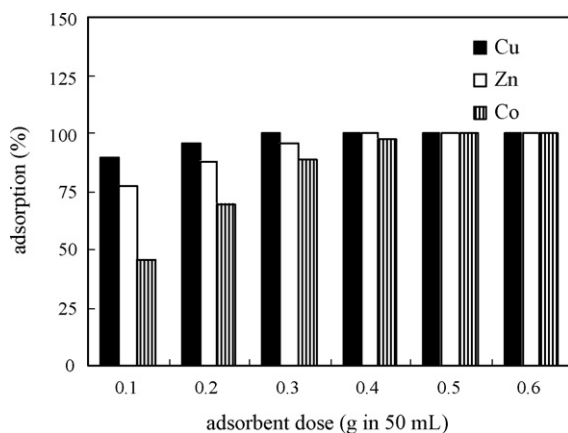


Fig. 9. Effect of adsorbent dose on the removal of Cu(II), Zn(II) and Co(II) ions from industry effluent samples by HA-Am-PAA-B.

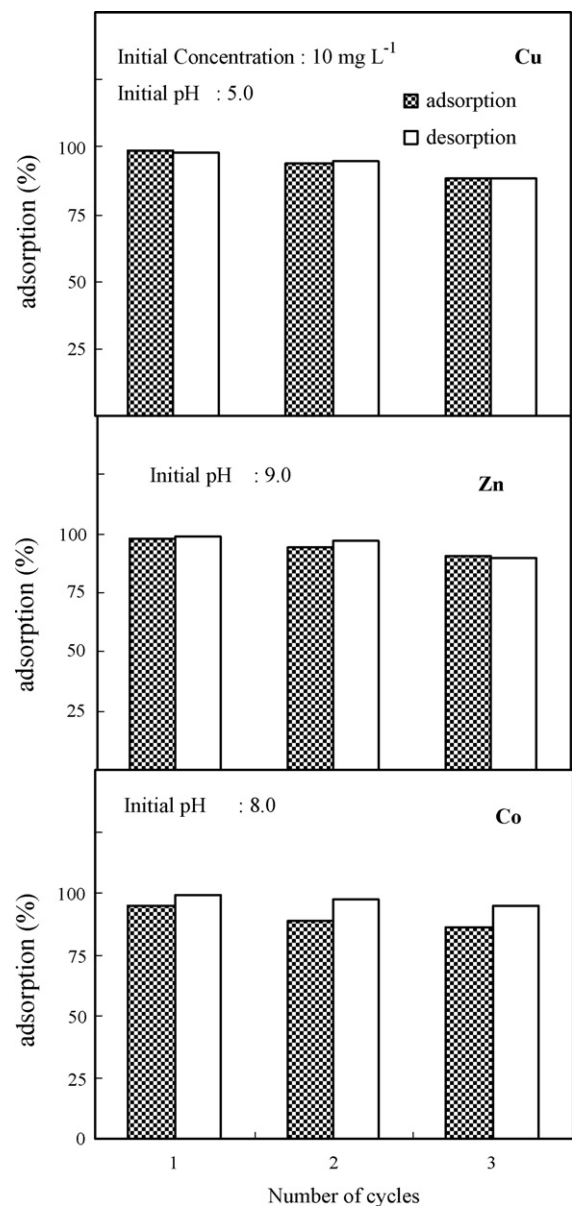


Fig. 10. Metal adsorption–desorption cycles with 0.1 M HCl as the desorbing agent.

respectively) was much higher than the reported values in literature. The values of Q^0 for the adsorption of Cu(II) ions were reported to be 2.23, 31.20, 32.17, 44.84, 56.55 and 86.0 mg g⁻¹ for adsorption onto tannic acid-immobilized activated carbon [27], methacrylic/acrylamide monomer mixture grafted fiber [28], 8-hydroxy quinoline immobilized bentonite [29], natural clay [1], unye bentonite [30] and granular activated carbon [31], respectively. Earlier workers reported the Q^0 values of 4.29, 7.88, 8.65, 8.02, 15.26, 30.73 and 49.94 mg g⁻¹ for the adsorption of Zn(II) ions onto natural clay [32], modified coir fiber [33], natural zeolite [34], modified jute fiber [35], biomass [36], sunflower stalks [37] and multiwalled carbon nanotube [38], respectively. The values of Q^0 for the adsorption of Co(II) ions onto kaolinite [39], sepiolite [40], magnesium silicate composite [41], styrene-g-polyethylene membrane [42], methacrylic acid/acrylamide monomer mixture grafted fiber [28], and aluminium pillared clay [43] were found to be 1.74, 7.57, 9.4, 25.0, 27.17 and 38.61 mg g⁻¹, respectively. The results are of greater environmental concern as HA-Am-PAA-B can be effectively applied to remove Cu(II), Zn(II) and Co(II) ions from industrial wastewater.

3.9. Desorption and regeneration studies

For an effective recycling process, adsorbed metal ions should be easily desorbed under suitable conditions without destroying the adsorbent material. In the first step, desorption experiments were performed using 0.1 M different reagents such as HCl, HNO₃, NaCl, CH₃COONa, NaOH, NaCO₃ and NaHCO₃ as desorption agents of which 0.1 M HCl gave better desorption results. The recovery studies were carried out in two steps. In the first step, desorption stability of 0.1 g HA-Am-PAA-B was determined in 50 mL 0.1 M HCl and no remarkable (<2%) desorbed humic acid was observed in the resulted solution by UV-vis spectrophotometer in three cycles. In the second step, recovery of adsorbed metal ions was studied. The results of desorption experiments are shown in Fig. 10. About 97.7, 98.5 and 99.2% of the adsorbed Cu(II), Zn(II) and Co(II) ions, respectively, were desorbed in the first cycle using 0.1 M HCl solution. This means that HCl solution breaks down the interaction forces between carboxyl group of HA-Am-PAA-B and metal ions. To show the reusability of spent adsorbent, adsorption-desorption cycle was repeated three times by using the same adsorbent. Even after three adsorption-desorption cycles, the removal and recovery capacities of HA-Am-PAA-B do not change significantly. The adsorbent can be reused almost without any significant loss in adsorption performance.

4. Conclusions

HA-Am-PAA-B is an effective adsorbent for the removal of Cu(II), Zn(II) and Co(II) ions from aqueous solutions. Metal removal increased with increase in pH and coordination bond formation with -COOH group of HA-Am-PAA-B was postulated as the mechanism for the removal of metal ions. The amount of metal ions adsorbed per unit weight of HA-Am-PAA-B at equilibrium time increased with increase in concentration. In the presence of Na and Ca-electrolyte, adsorption capacity of HA-Am-PAA-B towards metal ions decreased. A pseudo-second-order kinetic model agreed well with the kinetic behavior for the adsorption of metal ions. The equilibrium data fitted better with the Langmuir isotherm equation compared to the Freundlich and D-R equations. The findings indicated that the maximum amounts of metal ions adsorbed on HA-Am-PAA-B was found for Cu(II), followed by Zn(II) and Co(II). 0.3, 0.4 and 0.5 g of HA-Am-PAA-B completely removed Cu(II), Zn(II) and Co(II) ions, respectively, from 50 mL of simulated industrial wastewater. Regeneration experiments revealed quantitative desorption of adsorbed metal ions with 0.1 M HCl and the adsorbent can be reused for three cycles consecutively.

orption of adsorbed metal ions with 0.1 M HCl and the adsorbent can be reused for three cycles consecutively.

Acknowledgement

The authors are grateful to the Professor and Head, Department of Chemistry, University of Kerala, Trivandrum, for providing laboratory facilities for this work.

References

- [1] S. Veli, B. Alyuz, Adsorption of copper and zinc from aqueous solutions by using natural clay, *J. Hazard. Mater.* 149 (2007) 226–233.
- [2] The Council of the European Communities. Directive 82/176/EEC—on pollution caused by certain dangerous substances discharged into the aquatic environment of the community. *Off. J. Eur. Commun.* 1982, No. L 81/29.
- [3] D. Mohan, K.P. Singh, Single- and multi-component adsorption of cadmium and zinc using activated carbon derived from bagasse—an agricultural waste, *Water Res.* 36 (2002) 2304–2318.
- [4] U. Forstner, G.T.W. Wittman, *Metal Pollution in the Aquatic Environment*, vol. 2, Springer Verlag, Berlin, 1983, pp. 446–483.
- [5] A.T. Paulino, L.B. Santos, J. Nozaki, Removal of Pb²⁺, Cu²⁺ and Fe³⁺ from battery manufacturing wastewater by chitosan produced from silkworm chrysalides as a low-cost adsorbent, *React. Funct. Polym.* 68 (2008) 634–642.
- [6] A.D. Nikolaou, S.K. Golfinopoulos, T.D. Lekkas, M.N. Kostopoulou, DBP levels in chlorinated drinking water: effect of humic substances, *Environ. Monit. Assess.* 93 (2004) 301–319.
- [7] T.S. Anirudhan, M. Ramachandran, Synthesis and characterization of amidoximated polyacrylonitrile/bentonite composite for Cu(II), Zn(II) and Co(II) adsorption from solutions and industry wastewaters, *Ind. Eng. Chem. Res.* 47 (2008) 6175–6184.
- [8] T.S. Anirudhan, P.S. Suchithra, S. Rijith, Amine-modified polyacrylamide bentonite composite for the adsorption of humic acid in aqueous solutions, *Colloids Surf. A: Physicochem. Eng. Aspects* 326 (2008) 147–156.
- [9] H. Eccles, S. Hunt, *Immobilization of Ions by Biosorption*, Ellis Horwood Ltd., Chichester, UK, 1986.
- [10] C.H. Ho, N.H. Miller, Effect of humic acid on uranium uptake by haemetite particles, *J. Colloid Interface Sci.* 106 (1985) 281–288.
- [11] B.T. Abraham, T.S. Anirudhan, Sorption recovery of metal ions from aqueous solution using humus-boehmite complex, *Indian J. Chem. Technol.* 8 (2001) 286–292.
- [12] V.P. Vinod, T.S. Anirudhan, Adsorption behaviour of basic dyes on humic acid immobilized pillared clay, *Water Air. Soil Pollut.* 150 (2003) 193–217.
- [13] R.C. Mackenzie, A micro method for determination of cation exchange capacity of clay, *J. Colloid Interface Sci.* 6 (1951) 219–222.
- [14] R. James, G.A. Parks, P.J. Matpee, *Surface and Colloidal Science*, Plenum press, New York, 1998.
- [15] A. Ashok, B. Manas, P. Anjali, Removal of crystal violet dye from wastewater by surfactant-modified alumina, *Sep. Purif. Technol.* 44 (2005) 139–144.
- [16] J. Yu, M. Tong, X. Sun, B. Li, Biomass grafted with polyamic acid for enhancement of cadmium (II) and lead (II) biosorption, *React. Funct. Polym.* 67 (2007) 564–572.
- [17] A.F. Cotton, G. Wilkinson, *Advanced Inorganic Chemistry*, 3rd ed., Interscience Publishers, New York, 1972.
- [18] G. Crini, H.W. Peindy, F. Gimbert, C. Robert, Removal of C.I. basic green 4 (malachite green) from aqueous solutions by adsorption using cyclodextrin-based adsorbent: kinetic and equilibrium studies, *Sep. Purif. Technol.* 53 (2007) 97–110.
- [19] B.E. Eswed, F. Khalili, Adsorption of Cu(II) and Ni(II) on solid humic acid from the Azraq area, Jordan, *J. Colloid Interface Sci.* 299 (2006) 497–503.
- [20] S. Lagergren, *Kungliga Svenska Vetenskapsakademiens, Handlingar* 24 (1898) 1–39.
- [21] Y.S. Ho, G. McKay, Pseudo-second-order model for sorption process, *Process Biochem.* 34 (1999) 451–465.
- [22] M.F. Brigatti, C. Lugli, L. Poppi, Kinetics of heavy-metal removal and recovery in sepiolite, *Appl. Clay Sci.* 16 (2000) 45–57.
- [23] W. Reiman, H. Walton, *Ion-Exchange in Analytical Chemistry*, International Services of Monographs in Analytical Chemistry, Pergamon Press, Oxford, 1970, p. 38.
- [24] T.S. Anirudhan, P.G. Radhakrishnan, Thermodynamics and kinetics of adsorption of Cu(II) from aqueous solutions onto a new cation exchanger derived from tamarind fruit shell, *J. Chem. Thermodyn.* 40 (2008) 702–709.
- [25] S. Sirianuntapiboon, T. Hangsrisuwan, Removal of Zn²⁺ and Cu²⁺ by a sequencing batch reactor (SBR) system, *Bioresour. Technol.* 98 (2007) 808–818.
- [26] S. Rangaraj, S.H. Moon, Kinetics of adsorption of Co(II) removal from water and wastewater by ion exchange resins, *Water Res.* 36 (2002) 1783–1793.
- [27] A. Ucer, A. Uyanik, S.F. Aygun, Adsorption of Cu(II), Cd(II), Zn(II), Mn(II) and Fe(III) ions by tannic acid immobilized activated carbon, *Sep. Purif. Technol.* 47 (2006) 113–118.
- [28] R. Coskun, C. Soykan, M. Sacak, Adsorption of copper(II), nickel(II) and cobalt(II) ions from aqueous solution by methacrylic acid/acrylamide monomer mixture grafted poly(ethylene terephthalate) fiber, *Sep. Purif. Technol.* 49 (2006) 107–114.

- [29] O. Gok, A. Ozcan, B. Erdem, A.S. Ozcan, Prediction of the kinetics, equilibrium and thermodynamic parameters of adsorption of copper(II) ions onto 8-hydroxy quinoline immobilized bentonite, *Colloids Surf. A: Physicochem. Eng. Aspects* 317 (2008) 174–185.
- [30] E. Eren, Removal of copper ions by modified Unye clay, Turkey, *J. Hazard. Mater.* 159 (2008) 235–244.
- [31] H.J. Fan, P.R. Anderson, Copper and cadmium removal by Mn oxide-coated granular activated carbon, *Sep. Purif. Technol.* 45 (2005) 61–67.
- [32] N.Y. Dho, S.R. Lee, Effect of temperature on single and competitive adsorptions of Cu(II) and Zn(II) onto natural clays, *Environ. Monit. Assess.* 83 (2003) 177–203.
- [33] S.R. Shukla, S.P. Roshan, D.S. Amit, Adsorption of Ni(II), Zn(II) and Fe(II) on modified coir fibres, *Sep. Purif. Technol.* 47 (2006) 141–147.
- [34] E. Erdem, N. Karapinar, R. Donat, The removal of heavy metal cations by natural zeolites, *J. Colloid Interface Sci.* 280 (2004) 309–314.
- [35] S.R. Shukla, R.S. Pai, Adsorption of Cu(II), Ni(II) and Zn(II) on modified jute fibers, *Bioresor. Technol.* 96 (2005) 1430–1438.
- [36] S. Tunali, T. Akar, Zn(II) biosorption properties of *Botrytis cinerea* biomass, *J. Hazard. Mater.* B131 (2006) 137–145.
- [37] G. Sun, W. Shi, Sunflower stalks as adsorbents for the removal of metal ions from wastewater, *Ind. Eng. Chem. Res.* 37 (1998) 1324–1328.
- [38] L. Chungsyng, C. Huantsung, L. Chunti, Removal of Zinc(II) from aqueous solution by purified carbon nanotubes: kinetics and equilibrium studies, *Ind. Eng. Chem. Res.* 45 (2006) 2850–2855.
- [39] O. Yavuz, Y. Altunkaynak, F. Guzel, Removal of copper, nickel, cobalt and manganese from aqueous solution by kaolinite, *Water Res.* 37 (2003) 948–952.
- [40] M. Kara, H. Yuzer, E. Sabah, M.S. Celik, Adsorption of cobalt from aqueous solution onto sepiolite, *Water Res.* 37 (2003) 224–232.
- [41] A.D. Ebner, J.A. Ritter, J.D. Navratil, Adsorption of cesium, strontium and cobalt ions on magnetite and magnetite–silica composite, *Ind. Eng. Chem. Res.* 40 (2001) 1615–1623.
- [42] S.H. Choi, Y.C. Nho, Adsorption of Co^{2+} by styrene-g-polyethylene membrane bearing sulphonic acid groups modified by vanadium-induced graft copolymerization, *J. Appl. Polym. Sci.* 71 (1999) 2227–2235.
- [43] D.M. Manohar, B.F. Noeline, T.S. Anirudhan, Adsorption performance of Al pillared bentonite clay for the removal of cobalt(II) from aqueous phase, *Appl. Clay Sci.* 31 (2006) 194–206.